Challenging Glass 4 & COST Action TU0905 Final Conference – Louter, Bos & Belis (Eds)

The mechanical performance of adhesively bonded steel-glass composite panels: medium-scale tests and numerical models

S. Nhamoinesu & M. Overend
Glass & Façade Technology Research Group, University of Cambridge, United Kingdom

V.A. Silvestru & O. Englhardt
Institute of Building Construction, Graz University of Technology, Austria

ABSTRACT: Glass is often used in conjunction with steel framing but the two materials rarely act in a fully composite manner; the in-plane and out-of-plane loads on the framed glass structures are often resisted by the steel frame with the glass being used as infill panels. Steel-glass composite façade panels would increase structural and material efficiency as well as the aesthetical appeal. This paper investigates the mechanical performance of single-glazed and double-glazed medium-scale steel-glass composite panels subjected to flexural loads. The glass panels are linearly bonded to the reinforcing steel frames by Araldite 2047 adhesive, a two-part high strength acrylate. The paper also assesses the validity of two non-linear numerical models of the composite panels developed with different finite element analysis software. This research was undertaken at the University of Cambridge during a short-term scientific mission (STSM) supported by the COST Action TU0905.

1 INTRODUCTION

Contemporary architecture often encourages transparent facades with large glazed areas. Common systems consist of a frame made of steel or aluminium and glass panels which separate the inside of the building from the outside. While the in-plane and out-of-plane loads on the framed glass structures are mainly resisted by the steel frame, the glass is used as infill panels. Such glazing systems are not only structural inefficient due to their failure to fully utilize the load bearing potential of glass, they also lack aesthetical appeal due to the relatively large supporting frames. A solution to increase structural and material efficiency as well as to improve the aesthetical aspect is to design steel-glass composite façade elements. However, developing a steel-glass composite façade system presents a couple of engineering challenges: firstly, there are very few precedents on the use of glass as a primary load bearing material and secondly, there are no proven joining methods that allow efficient load transfer between glass and steel.

Investigations on the load-bearing behaviour of glass panels subjected to in-plane compression loads and in-plane shear loads, as well as combinations of in-plane loads and out-of-plane distributed loads have been conducted by different researchers with a variety of load transfer mechanisms between steel and glass. Linear adhesive bonding on the two shorter sides was used by Mocibob (2008), Wellershoff (2006) and Huveners (2009) analysed circumferential linear adhesive bonding and Wellershoff (2006) and Englhardt (2007) investigated the load transfer by contact at the glass edges near the panel corners through blocks made of grout or thermoplastics. However, in all cases there was no composite behaviour between the steel frame and the glass panel, but only an activation of the panel as a load bearing element. There have been studies conducted to investigate composite action between linearly bonded steel and glass Netusil (2012) and Louter (2012). However, these studies are primarily on the use of glass as a web in composite steel-glass beams.

To achieve composite action in a steel-glass façade element the transfer of high longitudinal shear forces between the components is necessary. Studies on adhesives performed at different research institutions Overend et al. (2010 and Belis et al. (2011) show which adhesive types are suitable for linear bonding. The over-arching conclusion from this work is that, while silicones are often used for structural sealant glazing systems to achieve flexible structural connections, stiffer adhesives like epoxies and acrylates are necessary for composite steel-glass elements. Nhamoinesu and Overend (2012) performed small-scale investigations to select a suitable adhesive for composite steel-glass elements based on criteria like cohesive or adherend failure preceded by substantial plastic strain in the adhesive, relatively high joint flexibility, adhesive shear strength of at least *7.5MPa* and a minimum loss of strength after exposure to temperature of up to *80°C*. The acrylate Araldite 2047 showed the best mechanical characteristics under short-duration testing and was therefore also used for the investigations presented in this paper.

2 FLEXURAL TESTS ON MEDIUM SCALE STEEL-GLASS COMPOSITE PANELS

2.1 *Specimen preparation & test procedure*

Three different specimen types (Figure 1) were assembled using *700mm* by *300mm* by *10mm* thick fully toughened glass panels manufactured to BS EN12150-2, these were adhesively bonded to *700mm* by *30mm* by *10mm* mild steel rectangular hollow sections (RHS) with a wall thickness of *1.5mm*. The bonding surface of the steel was sanded using *220* grit sandpaper; all surfaces were thoroughly cleaned with acetone before adhesive application. *3mm* thick PTFE-coated aluminium strips were placed on the ends of the steel profiles to act as spaces for the required 3mm adhesive thickness. A specially machined aluminium jig lined with a PTFE release film surrounded the perimeter of the glass panels to prevent the adhesive from flowing out of the joint during application as well as to align the steel hollow sections with the glass panels. Araldite 2047, a two-part high strength acrylate with a working time of approximately *11* minutes was applied to the edges of the glass using a manual dispensing gun. The assembled specimens were left to cure at ambient temperature and approximately *40%* relative humidity for at least 7 days before testing.
The following specimen types were tested:

- Type A – double glazed with one-way spanning steel RHS reinforcement linearly bonded to the long edges of the glass by *3mm* thick Araldite 2047 acrylate (Figure 1 left)
- Type A* – similar to Type A except that the steel RHS were not adhesively bonded but simply layered between two glass panels
- Type B – double glazed with two-way spanning steel RHS reinforcement linearly bonded around the full perimeter of the glass by *3mm* thick Araldite 2047 acrylate (Figure 1 middle)
- Type C – single glazed with one-way spanning steel RHS reinforcement linearly bonded to long edges of the glass by *3mm* thick Araldite 2047 acrylate (Figure 1 right)

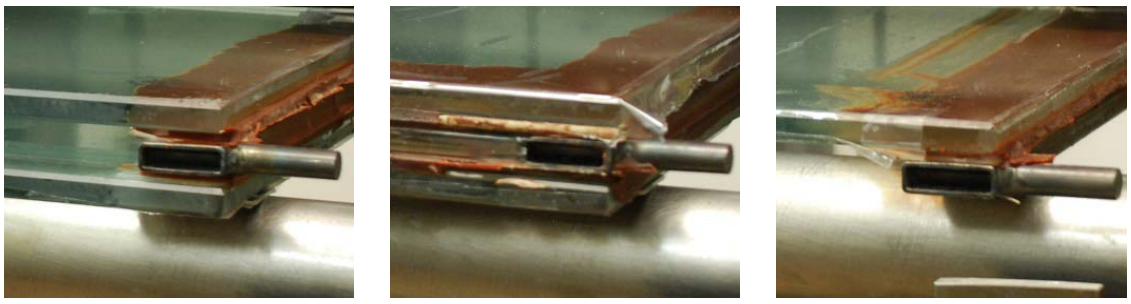

Figure 1. Different tested composite panels: Type A (left), Type B (middle) and Type C (right).

The specimens were subjected to four-point bending tests (Figure 2) on an Instron 5500R testing machine with a *150kN* load cell. Displacement transducers where placed to measure displacement of the glass at mid-span and the displacement of the loading bars. Four unidirectional strain-gauges were placed *3.5mm*, *50mm*, *100mm* and *150mm* from the long edge of

the glass respectively as shown in Figure 2. The gauges were used to measure the distribution of longitudinal normal stresses across the glass flange. Significant differences in the longitudinal normal stress in the glass would indicate shear lag, a phenomenon that is particularly pronounced in wide flanges. Another strain gauge was placed at the centre of the glass panel in order to measure the maximum normal stress in the glass at failure. The tests were displacement controlled with a displacement rate of *0.75mm/min*. Three specimens of each type were tested to destruction and all tests were performed at ambient temperature and approximately *40%* relative humidity.

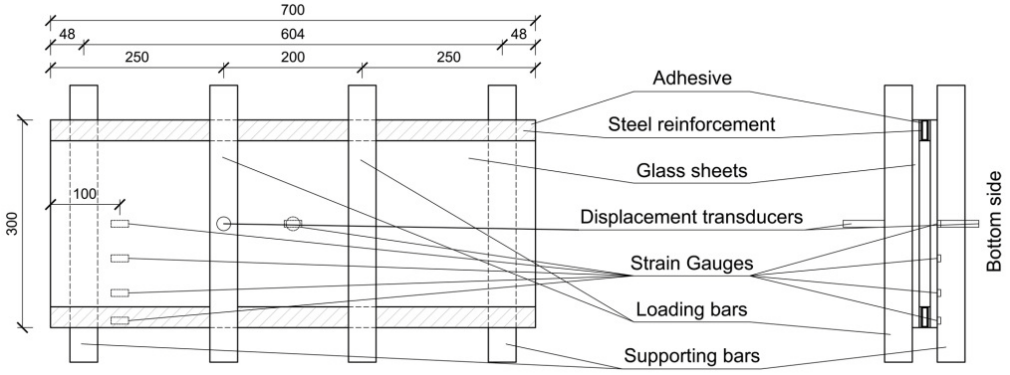

Figure 2. Dimensions of the composite panel (Type A) and position of supporting bars, loading bars, displacement transducers and strain gauges.

2.2 *Test results*

In all the Type A specimens, the bottom glass panel failed first (Figure 3) at loads ranging from *46.8kN* to *47.9kN* and centre displacements from *13.7mm* to *15.0mm* as shown in Table 1 and Figure 4. The test was continued after initial failure and mean post-fracture load of *22.2kN* was recorded before the top glass panel failed. The failure of the glass panels was explosive and as a consequence the composite panel could not be preserved as a whole element after failure. After the test, local whitening of the adhesive near the ends of the specimens was observed which suggests that plastic failure within the adhesive may have preceded glass failure. Measurements from the four strain-gauges placed across the width of the glass panels show higher longitudinal normal stresses in the regions of the glass near the steel RHS compared to the regions further away from the steel reinforcement (Figure 5); an indication of shear lag.

In the Type B specimens, the bottom glass panel failed first and in one specimen (B1), the top glass failed first. The initial failure loads ranged from *43.2kN* to *53.8kN* (Table 1) with a mean centre displacement of only *13mm* indicating that the two-way spanning specimens were much stiffer than the one-way spanning specimens. Failure of the second glass panel occurred at a mean load of *21.5kN*. The mode of failure was quite similar to that of Type A specimens with minor local adhesive whitening being observed after the test. It was possible to preserve the composite panel as a whole after failure of both glass panels as the steel RHS around the perimeter was successful in retaining the glass fragments. Strain-gauges placed across the width of the glass panels also indicated higher longitudinal normal stresses in regions of the glass near the steel reinforcement (Figure 5).

Four Type C specimens were tested. Three of them were prepared one month before testing, while specimen C4 was prepared six months before testing. The failure loads of the specimens ranged from *21.8kN* to *25.2kN* with a mean centre displacement of *22.4mm*. The age difference between specimens did not make any notable difference to their strength.

In the non-composite Type A* specimen, the bottom and top glass panels failed in quick succession with a maximum load of *20.5kN* (Figure 4), which is less than half the strength of the composite panel of similar geometry.

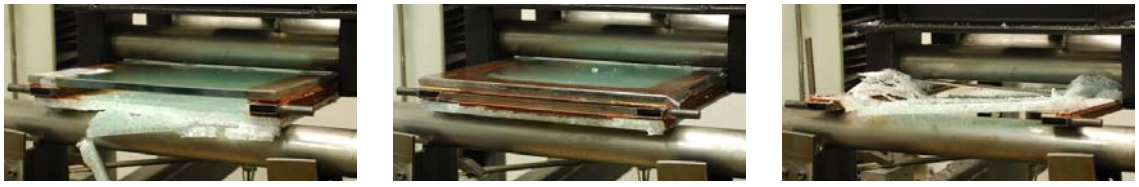

Figure 3. Test specimen for Type A (left), for Type B (middle) and for Type C (right) in four-point bending after initial glass failure.

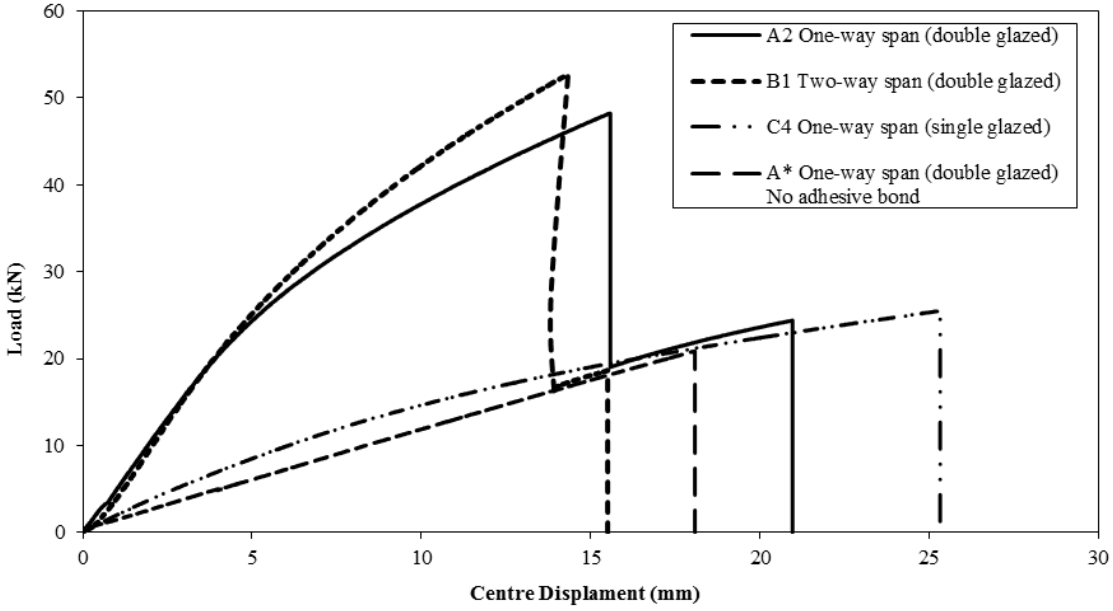

Figure 4. Centre displacement (*mm*) *vs.* load (*kN*) plots for steel-glass composite specimens subjected to four-point bending tests.

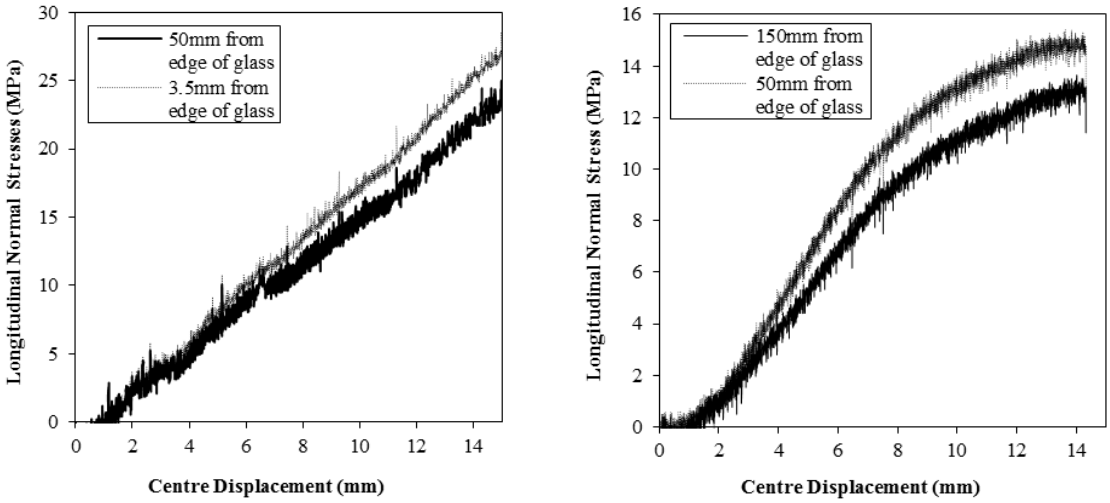

Figure 5. Plots of centre displacement (*mm*) *vs.* longitudinal normal stress in glass (*MPa*) for specimen A1 (left) and specimen B1 (right).

Table 1 below shows a summary of the results recorded from the tests.

Table 1. Summary of results for the composite panels tested.

Test specimen	Load at first fracture [*kN*]	Displacement at first fracture [*mm*]	Drop in load after first fracture [*kN*]	Failure load at fracture of second glass panel [*kN*]	Displacement at fracture of second glass panel [*mm*]
A1	45,8	15,0	31,0	19,5	17,6
A2	47,9	15,3	33,4	24,0	21,9
A3	45,9	13,7	31,7	23,2	20,9
A*	20,5	19,7	8,8	11,7	19,9
B1	52,3	14,2	36,6	18,3	17,6
B2	43,2	10,3	30,3	24,6	19,0
B3	53,8	14,5	37,4	21,7	17,3
C1	21,8	19,3	-	-	-
C2	24,3	24,3	-	-	-
C3	24,7	22,8	-	-	-
C4	25,2	23,1	-	-	-

3 NUMERICAL MODELING OF ADHESIVELY BONDED COMPOSITE PANELS

Two different finite element analysis software applications, LUSAS and ABAQUS, were used to numerically model the composite panels under four point bending test loading.

3.1 *The LUSAS numerical model*

A three-dimensional FEA model of the steel-glass composite Type C test was constructed using LUSAS v14.3 (Figure 6). A four node tetrahedral stress element type with linear interpolation order was used throughout the model. Since the composite panel is symmetrical about the mid-point of the glass in both the x and z axis, only a quarter of the composite panel was modelled. For the boundary conditions, one end of the steel hollow section was restrained in the y-direction. For the linear elastic model, the glass, the steel and the Araldite 2047 adhesive were all modelled as perfectly linear elastic materials with $E_{glass}=70GPa$, $v_{glass}=0.23$, $E_{steel}=209GPa$, $v_{steel}=0.3$, $E_{adhesive}=0.7GPa$ and $v_{adhesive}=0.47$. For the non-linear model, the steel was modelled as an elasto-plastic material. The adhesive was modelled as a visco-elastic material with de-coupled time-independent elasto-plastic and time-dependent viscoelastic properties. The time-dependent properties used can be described by the equation:

$$G(t) = G_v \times e^{-\beta t} = \left(G_0 - G_\infty\right) \times e^{-\beta t} \tag{1}$$

where the viscoelastic shear modulus $G_v = 211MPa$ and the viscoelastic decay constant $\beta = 0.002$ are determined from uniaxial tensile tests, Nhamoinesu and Overend (2012). A velocity $\dot{x}$ was applied on the line corresponding to the experimental load. A dynamic geometric and material non-linear analysis was run using the implicit method and an updated lagrangian approach.

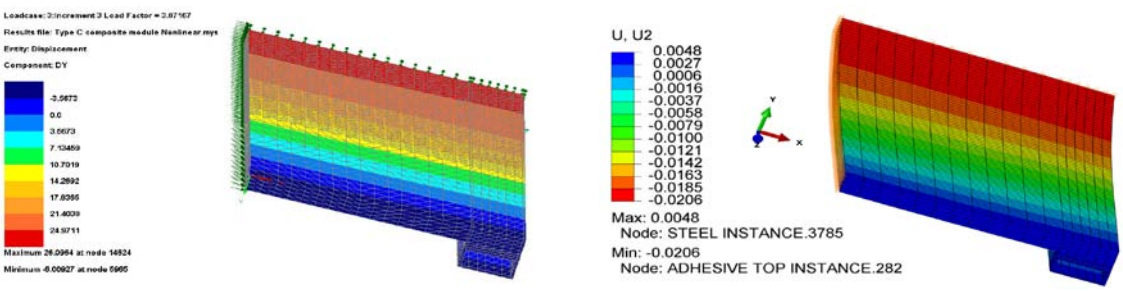

Figure 6. Displacement contour plot of the composite panel of Type C from LUSAS in mm (left) and from ABAQUS in m (right) for a principal stress in the glass of *140 MPa*.

3.2 *The ABAQUS numerical model*

A second three-dimensional FEA model for the composite Type C panel was developed using ABAQUS. Symmetry conditions about both the x and z axis were used to model only one quarter of the composite panel for computational efficiency. The supports in y direction were applied on a line at one end of the steel reinforcement at the position of the supporting bars from the test setup. The loading was modelled as a velocity according to the displacement controlled testing. For all the components 8-node linear brick elements with reduced integration (C3D8R) were used.

Firstly, a linear-elastic model was analysed. The same values for Young's modulus and Poisson's ratio for glass, steel and the adhesive as in the LUSAS model have been used. Then a non-linear analysis was performed. For this, the steel was modelled as an elastic perfectly plastic material. For the adhesive visco-elastic material properties were used. The viscoelastic properties are described in ABAQUS by a time dependent Prony series expansion of the dimensionless relaxation modulus $g_R(t)$:

$$g_R(t) = 1 - \sum_{i=1}^{N} g_i^P \left(1 - e^{-t/\tau_i^G} \right) \tag{2}$$

The series can be converted to

$$G_R(t) = G_0 \left(1 - \sum_{k=1}^{N} g_k^P \left(1 - e^{-t/\tau_k} \right) \right) \tag{3}$$

where G_0 is the instantaneous shear moduli determined from the values of the user-defined instantaneous elastic moduli E_0 and Poisson's ratio v_0. To determine the terms g_k^P and τ_k of the Prony series expansion MATLAB is used to fit a custom equation of the Prony series form to the shear modulus *vs.* time curve from the uniaxial relaxation tests performed at the University of Cambridge. This is not shown here for brevity. The instantaneous shear modulus is calculated to G_0*=300MPa* with the tensile modulus specified in the datasheet. A series with two terms was used due to the fact that only a small improvement is brought by more terms.

4 DISCUSSION

The 4-point bending tests of the different types of composite panels reveal that the stiffness of the two-way spanning double glazed panels and one-way spanning double glazed panels is initially identical up to a centre displacement of just over *5mm*. Beyond the *5mm* centre displacement mark, the two-way spanning panels become increasingly stiffer than the one-way spanning panels. In terms of strength, the mean failure load of the two-way spanning panels is approximately *7%* higher than that of the one-way spanning panels. This shows that for the aspect ratio tested, there is no significant gain in using two-way spanning panels especially if material cost is taken into consideration.

Type A, Type B and Type C composite panels achieve composite action due to the adhesive bonding, this is demonstrated by the poor performance shown by Type A* specimen where the glass panels were not adhesively bonded to the steel. This specimen showed less than half the strength of Type A composite panel specimens which have similar geometry.

The double glazed composite panels also exhibited significant post-fracture strength. After failure of one glass panel, both Type A and Type B specimens retained more than *40%* of the strength before failure. The post-fracture strength and stiffness behaviour of Type A and Type B specimens was nearly identical.

In these flexural tests, the behaviour of the composite panels could also be considered as that of composite beams in which the RHS steel profiles represent the web while the bottom and top glass panels represent wide flanges. Strain gauges placed across the width of the glass panels (flange) showed the evidence of shear lag. The longitudinal normal stresses near the steel profiles (web) were much higher than the stresses away from the steel profiles. This shear lag indi-

cates that the full width of the glass does not equally contribute to the composite action; there is therefore an effective width beyond which composite action between the steel web and the glass becomes negligible. Knowledge of the effective width and how to determine it is important in the design of full-scale composite panels subjected to out-of plane loading.

Simulation results from the LUSAS and ABAQUS numerical models were compared to experimental results (Figure 7).

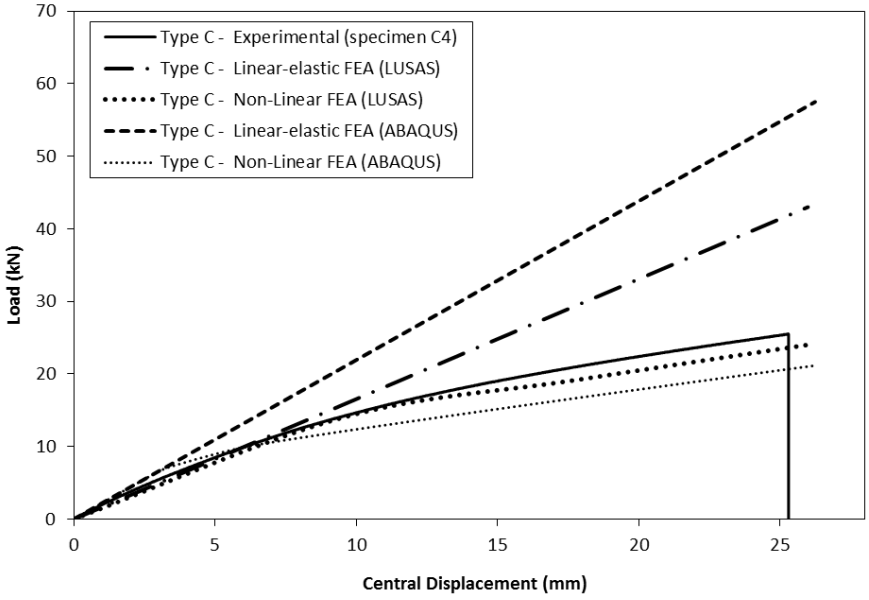

Figure 7. Displacement (*mm*) *vs.* numerical and experimental load (*kN*) plots for Type C composite panel.

The LUSAS non-linear model shows very good agreement with the experiment with a slight underestimation of stiffness at larger displacements when parts of the steel RHS are yielding. The linear-elastic model on the other hand shows good agreement for smaller loads as expected and its accuracy reduces beyond *10kN* loads as it fails to capture the plasticity in the steel and the adhesive.

The ABAQUS non-linear model shows reasonable agreement with the tests although the model initially overestimates the stiffness of the composite panel. The linear elastic model overestimates the stiffness considerably.

5 CONCLUSION

The experimental and numerical study on steel-glass composite panels described in this paper leads to the following conclusions:

- Glass panels linearly bonded to steel profiles by high strength adhesives are able to achieve composite action when subjected to flexural loads.
- Double glazed composite panels exhibit significant post-fracture strength.
- The gain achieved by using two-way spanning rather than one-way spanning composite panels may not be significant enough to compensate for the additional material and production costs.
- The use of wider glass panels results in shear lag when the composite panels are subjected to flexural loads. A way of determining the effective width of the glass (flanges) may be required when designing optimum composite panels.
- A visco-elastic non-linear numerical models constructed on LUSAS and on ABAQUS for Type C composite panels show reasonably good agreement with experimental test results.

The study presented in this paper forms the basis for future work where the numerical models will be extended to full-scale steel-glass composite panels.

6 ACKNOWLEDGEMENTS

The authors would like to acknowledge the support of the European Research Network on Structural Glass of the COST Action TU0905 for the Short-term Scientific Mission. The authors would also like to thank Pilkington NSG for providing all the glass used in this project.

REFERENCES

Belis, J., Van Hulle, A., Out, B., Bos, F., Callewert, D., Poulis, H. 2011. Broad screening of adhesives for glass-metal bonds. In *Glass Performance Days 2011*: 286-289. Tampere.

Englhardt, O. 2007. *Flächentragwerke aus Glas – Tragverhalten und Stabilität*. PhD Thesis. BOKU Vienna.

Haldimann, M., Luible A., Overend M. 2008. *Structural use of glass*. Structural Engineering Documents SED10. International Association for Bridge and Structural Engineering IABSE. Zurich.

Huveners, E.M.P. 2009. *Circumferentially Adhesive Bonded Glass Panes for Bracing Steel Frames in Facades*. PhD Thesis. Eindhoven University of Technology.

Louter, C., Belis, J., Bos, F., Veer, F. 2012. Reinforced glass beams composed of annealed, heat-strengthened and fully tempered glass. In *Challenging Glass 3 – Conference on Architectural and Structural Applications of Glass*: 691-702. Delft: IOS Press.

Mocibob, D., Crisinel, M. 2008. Linear connection system for structural application of glass panels in fully-transparent pavillons. In *Proceedings of Challenging Glass 1*. Delft, Netherlands.

Mocibob, D. 2008. *Glass panel under shear loading – use of glass envelopes for building stabilization*. PhD Thesis. Ecole Polytechnique Federale de Lausanne (EPFL).

Netusil, M., Eliasova, M., 2012. Structural design of composite steel-glass elements. In *Challenging Glass 3 – Conference on Architectural and Structural Applications of Glass*: 715-724. Delft: IOS Press.

Nhamoinesu, S., Overend, M. 2012. The mechanical properties of adhesives for a steel-glass composite façade system. In *Challenging Glass 3 – Conference on Architectural and Structural Applications of Glass*: 293-306. Delft: IOS Press.

Overend, M., Jin, Q., Watson, J. 2010: *Investigations into steel-glass adhesive joints*. Technical Report Number CUED/D-STRUCT/TR231. University of Cambridge.

Wellershoff, F. 2006. *Nutzung der Verglasung zur Aussteifung von Gebäudehüllen*. PhD Thesis. RWTH Aachen.

ABAQUS 6.10. 2010. *Analysis User's Manual, Volume III: Materials*. Dassault Systems.

LUSAS Finite Element System. 2012. *Lusas theory manual*. FEA Ltd. United Kingdom.